Desalination and Water Treatment
www.deswater.com
doi: 10.5004/dwt.2023.30120

315 (2023) 139–149
December

Comparison of oxytetracycline adsorption on semi-carbonized acrylic fibers under different orthogonal modifications

Wen-bin Li[a,†], Chu-tong Yu[a,†], Hong-yan Deng[a,*], Touqeer Abbas[b], Li-na Wen[c], Xue-fei Xiong[d]

[a]*College of Environmental Science and engineering, China West Normal University, Nanchong Sichuan 637009, China, emails: dhongyan119@163.com (H.-y. Deng), lwb062@163.com (W.-b. Li), 3336249772@qq.com (C.-t. Yu)*
[b]*Department of Soil, Water, and Climate, University of Minnesota, Twin 637009, USA, email: abbastouqeer@yahoo.com*
[c]*Sichuan Highway Planning, Survey, Design and Research Institute Ltd., Chengdu 610041, China, email: 26879619@qq.com*
[d]*Sichuan Chuanqian Expressway Co., Ltd., Gulin 646500, China, email: 11022265@qq.com*

Received 17 August 2023; Accepted 6 November 2023

ABSTRACT

In this study, sodium alginate (SA), dimethyl dodecyl betaine (BS), and chitosan (CS) were used for single, binary, and ternary modifications on the surface of semi-carbonized fibers (Sf) prepared using acrylic fiber. Batch method was used to investigate the adsorption characteristic of oxytetracycline (OTC) on the tested materials, and the effects of pH, temperature, and ionic strength on oxytetracycline adsorption were compared. The structural particularities of the tested materials was studied using scanning electron microscopy (SEM) and Fourier-transform infrared spectroscopy (FTIR). Results showed that: (1) Langmuir model can better fitted the adsorption isotherms of OTC than Henry and Freundlich models, with the maximum adsorption capacity (q_m) maintained at 16.11–65.25 mmol/kg. The q_m of oxytetracycline presented the trend of ternary > binary > single modification. (2) In the pH range of 1–9 and ionic strength range of 0.01–0.5 mol/L, the adsorption amount of OTC on different modified Sfs increased first and then decreased with increasing pH and ionic strength, reaching the maximum value at pH 5 and ionic strength of 0.1 mol/L. (3) OTC adsorption on different modified Sfs increased with the increase in temperature, and the adsorption was a spontaneous, endothermic, and entropy-increasing process, which conformed to the pseudo-second-order kinetic equation. (4) SEM and FTIR results proved that the modifiers were modified on the surface and that they changed the surface properties of Sf. The adsorption amount of OTC on 100SA/BS/CS-Sf still reached about 50% of the original material after three times of regeneration.

Keywords: Semi-carbonized fiber; Oxytetracycline; Chitosan; Dimethyl dodecyl betaine; Sodium alginate

1. Introduction

Rapid societal change has posed difficulties to the aquatic environment, with new pollutants altering, growing, and frequently being found at higher-than-predicted concentrations [1]. Due to the aquaculture industry's recent rapid growth, antibiotics are frequently employed to cure and prevent animal infections, and their usage is on the rise [2,3]. However, the abuse of antibiotics poses a significant threat to the ecological environment because their metabolites, which cannot fully disintegrate in the animal body, penetrate the environment of surface waters and result in catastrophic water contamination [4]. Antibiotic resistance is induced in pathogenic bacteria, and it leads to major environmental issues, making it one of the most pressing issues in the water environment. Antibiotics also alter the structure and

* Corresponding author.
† These authors have contributed equally to this work and share first authorship.

function of microbial communities in the ecosystem [5]. The typical tetracycline antibiotic oxytetracycline (OTC) is used in huge amounts because of its low cost, effective performance, and low toxicity, and its presence in natural waters is importantly increasing [6].

Antibiotics may currently be removed effectively through biological degradation, membrane separation, adsorption, and enhanced oxidation. Due to its usually straightforward operation, effective therapeutic effect, and lack of production of harmful metabolites, adsorption is typically used to adsorb antibiotics in polluted water [7]. The commonly used antibiotic adsorbents include carbon materials, polymers, minerals, and nanomaterials [8–11]. However, some of the materials have a more restricted range of applications because of their prolonged preparation time, challenging manufacturing method, and high production costs. People have started looking for less expensive and more efficient adsorption materials, including waste products from daily life, (e.g., peanut shells, pomelo peels, and wheat straws) [12–14], to replace the expensive adsorbents. Carbon materials have drawn considerable attention recently due to their substantial surface area and superior adsorption capabilities. Hu et al. [15] used bagasse to produce biochar with the advantages of low cost, simple process, and high adsorption efficiency, and the maximum adsorption capacity of the biochar carbonized at 500°C for sulfamethoxazole and ciprofloxacin antibiotics could be up to 53.3 and 54.5 mg/g, respectively. Yu et al. [16] modified biochar with potassium acetate and obtained a specific surface area (1,147.80 m^2/g) higher than that of pyrolyzed biochar. The adsorption of OTC by the modified biochar could reach 165 mg/g at the solution pH of 3–8. Zhou et al. [17] prepared two kinds of unmodified and phosphoric acid-modified biochar and used them to remove amoxicillin in water. The phosphoric acid-modified biochar adsorbed 50 mg/L amoxicillin, the adsorption equilibrium could be reached within 60 min, and removal efficiency of amoxicillin was as high as 96.0%, and the maximal adsorption capacity was as high as 198.8 mg/g at 65°C.

The modified biochar has more good adsorption sites for antibiotics, and it demonstrated improved antibiotic adsorption [18]. It also has more effective sites for antibiotic adsorption. Composite modification improves the performance of carbon-based materials more effectively than the modifiers employed alone or in combination [19]. The straw biochar modified with sodium bicarbonate and melamine had a superior adsorption capacity for tetracycline. It can remove tetracycline quickly and efficiently in a short time and the maximum adsorption amount reached 347 mg/g [20]. Ma et al. [21] prepared sludge biochar modified with Fe/Zn, H_3PO_4, and a combination of the two (Fe/Zn + H_3PO_4). The results showed that the Fe/Zn + H_3PO_4-modified biochar with high adsorption capacity is a promising adsorbent for fluoroquinolones and other antibiotics. Three antibiotics in water, namely, ciprofloxacin, norfloxacin, and ofloxacin, showed excellent adsorption performance, with maximum adsorption capacities of 83.7, 39.3, and 25.4 mg/g, respectively [21].

Fibers are effective adsorbent materials due to their porous structure and large surface area. Studies found that fiber materials have a faster adsorption rate and higher adsorption capacity for heavy metal ions [22]. When used for adsorption of pollutants, carbonized fiber has the advantages of a large surface area, abundant pore structure and active sites, broad spectrum, sustainability, and degradability. The adsorption capacity of carbonized fibers could be greatly improved if multiple composite modification is carried out. Few related studies and reports on this topic were published. In the present work, sodium alginate (SA), dimethyl dodecyl betaine (BS), and chitosan (CS) were used for single, binary, and ternary modifications on the surface of semi-carbonized fiber (Sf) prepared using acrylic fiber. Batch method was used to investigate the adsorption characteristic of OTC on the tested materials, and the effects of pH, temperature, and ionic strength on oxytetracycline adsorption were compared. The structural particularities of the tested materials was studied by using scanning electron microscopy (SEM) and Fourier-transform infrared spectroscopy (FTIR). This research aims to provide a theoretical basis for the development of composite-modified carbonized fibers for the adsorption of antibiotic contaminants.

2. Materials and method

2.1. Experimental materials

BS (purchased from Tianjin Xingguang Auxiliary Factory, China, analytic reagent), SA (purchased from Chengdu Cologne Chemical Co., Ltd., China, analytic reagent), and CS (purchased from Shanghai Yuanye Biotechnology Co., Ltd., China, analytic reagent) with 90% purity were used as the modifiers. The molecular formula of the three modifiers is shown in Fig. 1.

Acrylic fiber was soaked in deionized water for 24 h and subsequently decolorized using ethanol. After decolorization, the raw material was placed in a muffle furnace at 300°C and stored in an anaerobic environment for 2 h. Following cooling, the material was ground through a 60-mesh screen to obtain Sf. A certain weight of Sf was prepared for single modification, slowly added to the prepared BS (CS and SA are similar) solution with a Sf/water ratio of 1:10, and then dispersed by ultrasound at 60°C for 3 h. The samples were centrifuged at 4,800 rpm for 20 min, and the supernatant was separated. After being washed three times with deionized water, the samples were dried at 60°C for 12 h and then passed through a 0.25 mm sieve. BS-modified Sf (BS-Sf), CS-modified Sf (CS-Sf), and SA-modified Sf (SA-Sf) were obtained. The binary and ternary modifications were the same as the single modification, in which singly modified Sf was modified by other two modifiers individually and simultaneously. Then, CS-modified BS-Sf (BS/CS-Sf), SA-modified BS-Sf (SA/BS-Sf), CS-modified SA-Sf (SA/CS-Sf), CS-modified SA/BS-Sf (SA/BS/CS-Sf) could be obtained.

The dosage of BS, SA, and CS were calculated using Eq. (1):

$$W = m \times \mathrm{CEC} \times M \times 10^{-6} \times \frac{R}{b} \tag{1}$$

where W (g) is the quantity of modifier. m (g) represents the mass of the material that will be modified. CEC (mmol/kg) denotes the cation exchange capacity of Sf. M (g/mol) refers to the molecular mass of the modifier. R is the modified

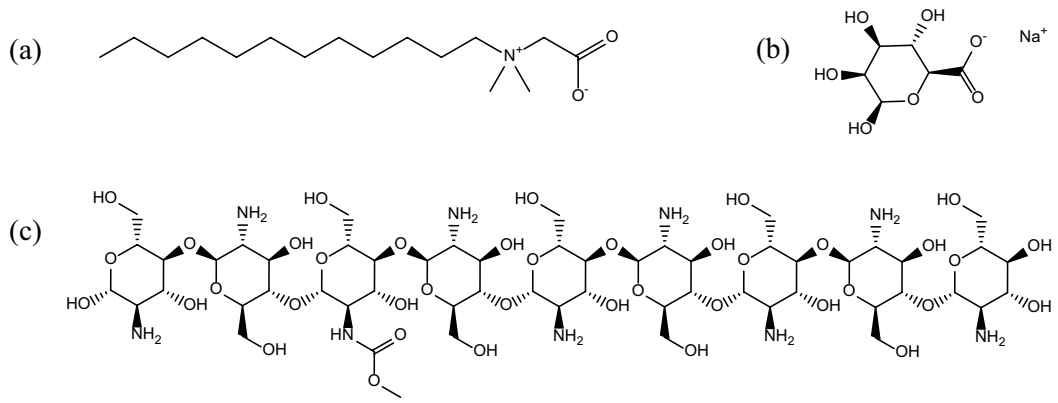

Fig. 1. Molecular structural formulas of BS (a), SA (b), and CS (c).

proportion. *b* stands for the content of the modifier product (mass fraction).

The test contaminant OTC was purchased from Sigma, USA, with a purity of 99.9%. The hygromycin molecule has three pKa (pK_1 = 3.57, pK_2 = 7.49, pK_3 = 9.44) [23]. At pH < 5.5, oxytetracycline is mainly present as cations and amphoteric ions, at 5.5 < pH < 8.7, it is mainly present as amphoteric ions and amidated anions, and at pH > 8.7, amidated and divalent anions are predominant [24].

2.2. Experimental design

The structural particularities of the tested materials was studied by using SEM and FTIR detection. The concentrations of OTC were set to ten concentration gradients of 0, 0.3, 0.6, 1.2, 3, 6, 12, 18, 24, and 30 mg/L. The temperature was set to 25°C, the pH of the solution was set to 5, and the ionic strength was set to 0.1 mol/L of NaCl.

Temperature is set at 25°C, 35°C and 45°C (pH value of the solution: 5; ionic strength: 0.1 mol/L). pH values are set at 1, 3, 5, 7 and 9 (initial solution temperature: 25°C; ionic strength: 0.1 mol/L). Ionic strength was set at 0.01, 0.1, 0.2 and 0.5 mol/L (pH value of the solution: 5; initial solution temperature: 25°C).

The adsorption time was set as 5, 10, 30, 60, 120, 180, 240, 300, 360, 480, and 720 min. The temperature was set as 25°C, the pH value of the solution was set as 5, and the ionic strength was set as 0.1 mol/L of NaCl.

2.3. Experimental methods

S_{BET} were analyzed using a multipoint Brunauer–Emmett–Teller method through the Gold APP V-Sorb 2800P analyzer (Ultrametrics, Beijing, China). SEM was performed using the Japanese Hitachi S-4800 scanning electron microscope. FTIR analysis was performed on the Nicolet iS50 type Fourier-transform infrared spectrometer (Thermo Fisher, Massachusetts, USA).

The batch equilibrium method was used for OTC adsorption. A total of 0.1000 g of the sample was weighed in nine 50-mL plastic centrifuge tubes to which 20 mL of oxytetracycline solutions with different concentration gradients were respectively added. The samples were oscillated at 20°C and 200 rpm for 12 h at constant temperature and centrifuged at 4,800 rpm for 10 min [18]. The concentration of the OTC in the supernatant was determined by high-performance liquid chromatography (Thermo Fisher, Massachusetts, USA) with the wavelength of 273 nm, and the equilibrium adsorption amount was calculated by the subtraction method. All the above measurements were substituted into the standard solution for analytical quality control.

2.4. Data processing

Equilibrium adsorption capacity was calculated according to Eq. (2).

$$q_e = \frac{V \times \left(c_0 - c_e\right)}{m} \tag{2}$$

where c_0 and c_e are the initial concentration and equilibrium concentration of OTC in solution, respectively (mmol/L). V refers the volume of oxytetracycline solution added (mL). m is the mass of the tested sample (g). q indicates the equilibrium adsorption capacity of oxytetracycline on the tested sample.

The Langmuir, Freundlich, and Henry model were used to fit the adsorption isotherm of oxytetracycline, as shown in Eqs. (3)–(5).

$$q_e = \frac{q_m b c_e}{1 + b c_e} \tag{3}$$

$$q_e = k c_e^{(1/n)} \tag{4}$$

$$q_e = K c_e \tag{5}$$

where q_m is the maximum adsorption amount of oxytetracycline for the tested sample, mmol/kg; b and n are the apparent equilibrium constant of oxytetracycline adsorption on the tested sample for the measurement of adsorption affinity. k is a parameter related to the adsorption capacity. K represents the distribution coefficient of oxytetracycline in solid phase adsorbent and solvent, and also represents the OTC binding capacity of the tested sample to a certain extent.

Parameter K in the Henry model is equivalent to the apparent adsorption constant of equilibrium constant,

and called the apparent thermodynamic parameters [25] Eqs. (6)–(8):

$$\Delta G = -RT\ln K \tag{6}$$

$$\Delta H = R\left(\frac{T_1 \cdot T_2}{T_2 - T_1}\right)\cdot \ln\left(\frac{K,T_2}{K,T_1}\right) \tag{7}$$

$$\Delta S = \frac{\Delta H - \Delta G}{T} \tag{8}$$

where ΔG is the standard free energy change (kJ/mol), R is a constant (8.3145 J/mol·K), T is the adsorption temperature (T_1 = 298.16 K, T_2 = 318.6 K), ΔH is the enthalpy of adsorption process (kJ/mol), and ΔS is the entropy change of adsorption process (J/mol·K).

The pseudo-first-order and pseudo-second-order kinetics equation models were used to simulate the adsorption process of oxytetracycline on the tested materials [26]. The kinetics equations were defined as Eqs. (9)–(10):

$$\ln\left(q_e - q_t\right) = \ln q_e - k_1 t \tag{9}$$

$$\frac{t}{q_t} = \frac{1}{q_e^2 k_2} + \frac{t}{q_e} \tag{10}$$

where q_t (mmol/kg) is the adsorption capacity corresponding to the adsorbent at time t; k_1 (min^{-1}) and k_2 (mmol/kg·min) are pseudo-first-order and pseudo-second-order reaction rate constants, respectively; t is the adsorption time (min).

CurveExpert 1.4 fitting software was used in isothermal fitting, and Origin 2022 was adopted to improve data plotting. The data were expressed as the means with standard deviation, and different letters indicate significant differences among various amendments. Analysis of variance was performed to determine the effects of amendments, followed by Tukey's honestly significant difference test. Differences of $P < 0.05$ were considered significant.

3. Results and discussion

3.1. Isothermal adsorption of oxytetracycline on different modified Sfs

The adsorption isotherms of OTC on each modified Sf under the conditions of 25°C, pH 5, and ionic strength of 0.1 mol/L are shown in Fig. 2a–d. The OTC adsorption capacity of the different modified Sfs increased with the increase in equilibrium concentration, showing L-shaped adsorption curves. The Langmuir, Henry, and Freundlich models were used to fit the adsorption isotherms of OTC by the modified Sfs (Table 1), and the fitting correlation reached a highly significant level ($P < 0.01$). The fitting effect of the

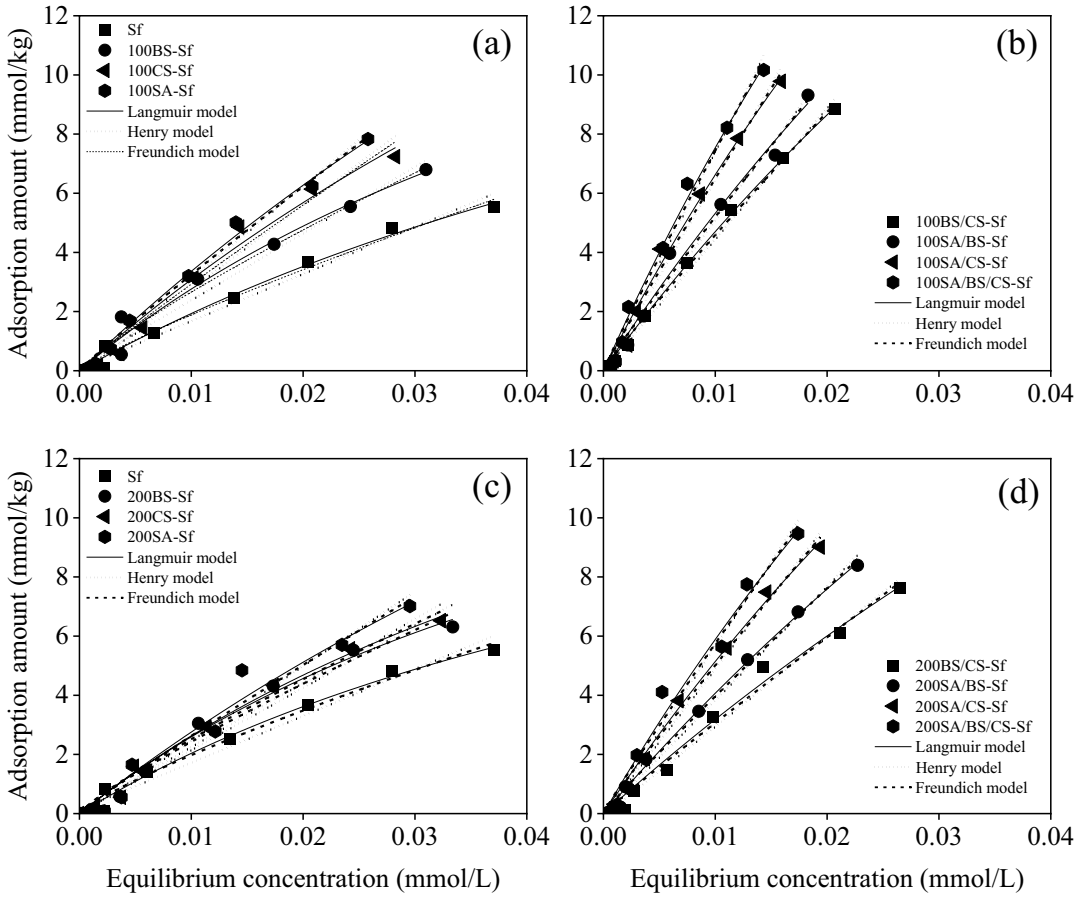

Fig. 2. Adsorption isotherms of oxytetracycline by 100% (a,b) and 200% (c,d) modified Sfs.

Table 1
Fitting parameters by Langmuir, Henry, and Freundlich models

Tested samples	Langmuir model			Henry model			Freundlich model		
	q_m	b	r	K	K_r	r	k	n	r
Sf	16.11	14.47	0.9952**	163.82	–	0.9871**	97.43	1.17	0.9935**
100BS-Sf	21.25	14.93	0.9914**	231.56	1.41	0.9855**	127.04	1.19	0.9903**
100CS-Sf	36.49	9.22	0.9909**	279.35	1.71	0.9877**	218.87	1.07	0.9886**
100SA-Sf	47.00	7.70	0.9960**	311.78	1.90	0.9945**	245.85	1.06	0.9952**
100BS/CS-Sf	53.96	9.55	0.9990**	444.68	2.71	0.9975**	333.74	1.07	0.9983**
100SA/CS-Sf	57.76	10.15	0.9943**	508.47	3.10	0.9931**	218.49	1.07	0.9983**
100SA/BS-Sf	60.46	12.31	0.9949**	643.64	3.93	0.9932**	510.97	1.06	0.9938**
100SA/BS/CS-Sf	65.25	13.06	0.9951**	741.49	4.53	0.9936**	595.10	1.05	0.9940**
200BS-Sf	19.01	15.81	0.9915**	212.59	1.30	0.9816**	124.11	1.17	0.9866**
200CS-Sf	21.30	14.08	0.9959**	220.64	1.35	0.9891**	127.21	1.17	0.9935**
200SA-Sf	35.88	8.32	0.9837**	249.37	1.52	0.9812**	194.80	1.07	0.9821**
200BS/CS-Sf	52.66	6.44	0.9942**	298.06	1.82	0.9930**	254.47	1.04	0.9933**
200SA/CS-Sf	56.61	7.74	0.9973**	384.30	2.35	0.9962**	304.73	1.06	0.9967**
200SA/BS-Sf	57.24	9.87	0.9978**	490.18	2.99	0.9963**	380.62	1.06	0.9969**
200SA/BS/CS-Sf	60.40	10.80	0.9901**	567.21	3.46	0.9887**	454.88	1.05	0.9892**

Note: **indicates significance at $P = 0.01$ level ($r = 0.765$ at $P = 0.01$ when the degree of freedom $f = 8$).

Langmuir model was better than that of the Freundlich and Henry models, indicating that the adsorption of OTC on the modified Sfs highly conformed to the Langmuir model. The maximum adsorption capacity (q_m) values of OTC on the modified Sfs were 16.11–65.25 mmol/kg, ranking in the order of ternary > binary > single > non-modification, which is consistent with the trend of adsorption isotherms in Fig. 2. This result indicated that BS, CS, and SA modifications increased the OTC adsorption capacity of Sf, consistent with the result of previous studies on single and composite modifications [27].

The adsorption amounts of OTC on different modified Sfs were 1.32–4.05 (100% modification) and 1.18–3.75 (200% modification) times higher than that on raw Sf, indicating that the organic phase on the Sf surface partly affected the adsorption of oxytetracycline. The parameters k of the Freundlich model and K of the Henry model followed the same trend as the q_m of the Langmuir model. The adsorption affinity (n) of the Freundlich model was lower than the b of the Langmuir model. These results indicated that the test materials had homogeneous surfaces, the adsorption sites on the material surface were uniformly distributed, and the adsorption was monolayer adsorption [28]. The adsorption amount of the material used, which was a kind of antibiotic adsorption material with good performance, was several times higher than of those of nanohydroxyapatite and Mg-loaded amphoteric clay [29,30].

3.2. Effect of pH and ionic strength oxytetracycline adsorption

The adsorption amount of OTC on each modified Sf increased first and then decreased with the increase in pH when the pH was in the range of 1–9 (Fig. 3a–d), reaching the maximum at pH 5. When the pH increased from 1 to 5, the adsorption amount of OTC on the modified Sfs increased by 61.28%–244.47% (100% modification) and 41.29%–214.13% (100% modification). The pH of the solution had a great influence on the antibiotic adsorption, may be due to the existence of antibiotics in the aqueous solution. oxytetracycline has three different pKa, and it exists in three different main forms under different pH conditions: cationic OTC^+ (pH < 3.57), neutral molecule OTC^0 (pH between 3.57 and 9.44), and anionic OTC^- (pH > 9.44) [31]. Therefore, under pH 5, antibiotics can be combined with modified Sfs by cation exchange and hydrophobic bond. With increasing pH, the proportion of negative charge in the antibiotic molecule increased, and the adsorption decreased gradually [32].

When the ionic strength changed from 0.01 to 0.5 mol/L, the adsorption amount of oxytetracycline on the modified Sfs increased first and then decreased (Fig. 4), reaching the peak value at 0.1 mol/L. When the ionic strength increased from 0.01 to 0.1 mol/L, the adsorption amounts of OTC on the modified Sfs were 1.01–1.21 (100% modification) and 0.91–1.17 (200% modification) times higher than that on Sf, mainly due to the low electrolyte content in the solution when the ion concentration is 0.01–0.1 mol/L. With the increase in ion concentration, the electrical conductivity of the solution enhanced, and the Na^+ content in the solution gradually increased; the surface charge of the tested samples was compressed to form a negative compressed double-electron layer structure [33], which changed the electrostatic potential of the adsorption surface of the modified Sfs and led to the increase in the adsorption amount of oxytetracycline. Considering that the concentration of NaCl in the solution was too high, oxytetracycline was not easily released, making the antibiotics less soluble, which also led to a decrease in the amount of oxytetracycline adsorbed.

3.3. Influence of temperature on oxytetracycline adsorption

The influence of temperature on the adsorption of OTC by different modified Sfs is shown in Fig. 5. As the temperature

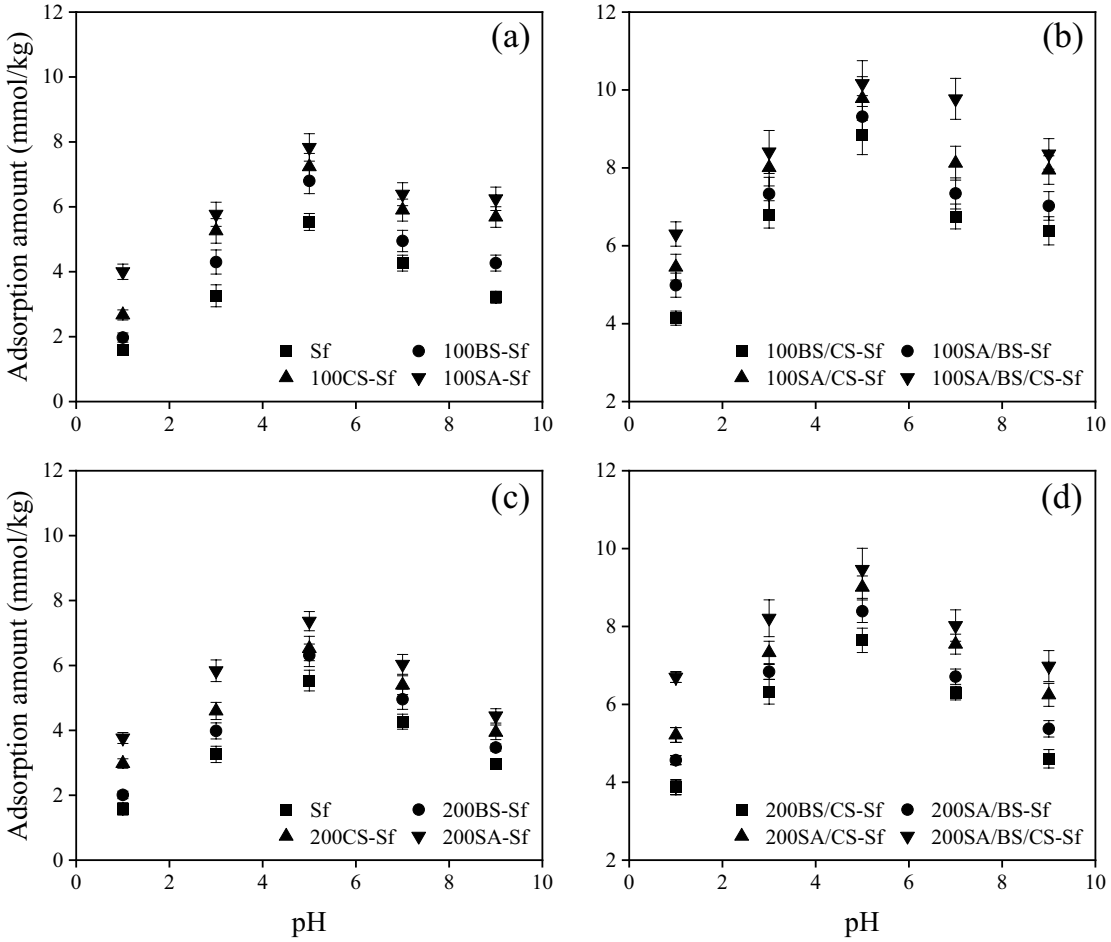

Fig. 3. Effect of pH on oxytetracycline adsorption by 100% (a,b) and 200% (c,d) modified Sfs.

increased from 15°C to 45°C, the adsorption amount of oxytetracycline by the modified Sfs increased, indicating a positive temperature effect. The adsorption amounts of OTC by single, binary, and ternary modified Sfs increased by 11.85%–67.56%, 8.67%–15.87%, and 8.61%–9.49%, respectively. The thermodynamic parameters of oxytetracycline adsorption by different modified Sfs are shown in Table 2. The Gibbs free energy variation (ΔG) of Cd(II), Pb(II), and Zn(II) adsorption by different modified Sfs under the conditions of 15°C and 45°C were less than 0, thus indicating that the adsorption process was spontaneous. Furthermore, the spontaneity was stronger at 45°C under the same treatment. The enthalpy change (ΔH) of metal ion adsorption on the modified Sfs was positive, indicating that the adsorption process was endothermic, and temperature increase was conducive to their adsorption of OTC, which is consistent with the positive temperature effect shown in Fig. 5.

As the temperature increased, the rate of diffusion of oxytetracycline molecule in the solution increased, and the chance of contact between OTC and the modified Sfs increased [34]. A higher temperature corresponds to a better adsorption effect of the modified Sfs on oxytetracycline. The results can be mainly attributed to the chemical reaction of ion exchange and complexation [35]. The entropy changes (ΔS) of OTC adsorption in all tested Sfs were greater than 0, indicating that the adsorption process was an entropy-increasing reaction, mainly due to the different oxytetracycline adsorption mechanisms of the modified Sfs, leading to increased system confusion [36]. The adsorption process may involve physical (electrostatic attraction) and chemical reactions (complexation, ion exchange, and precipitation).

3.4. Adsorption kinetic characteristics of oxytetracycline by different tested materials

The adsorption kinetics curves of OTC on different modified Sfs are shown in Fig. 6. At the early stage of adsorption, the adsorption removal of oxytetracycline by the test materials was rapid, and the adsorption amount increased dramatically. Then, the adsorption rate decreased slowly as the adsorption proceeded. It finally reached equilibrium at 120 min, because in the early stage of adsorption, the test material was filled with a large number of adsorption sites, and OTC was rapidly adsorbed onto the surface of the modified Sfs. With the increase in the adsorption of oxytetracycline on the material surface, the adsorbed sites reached saturation, the OTC molecules migrated from the surface to the interior. With the increase in resistance to diffusion, the rate of growth of the amount of adsorption gradually reduced.

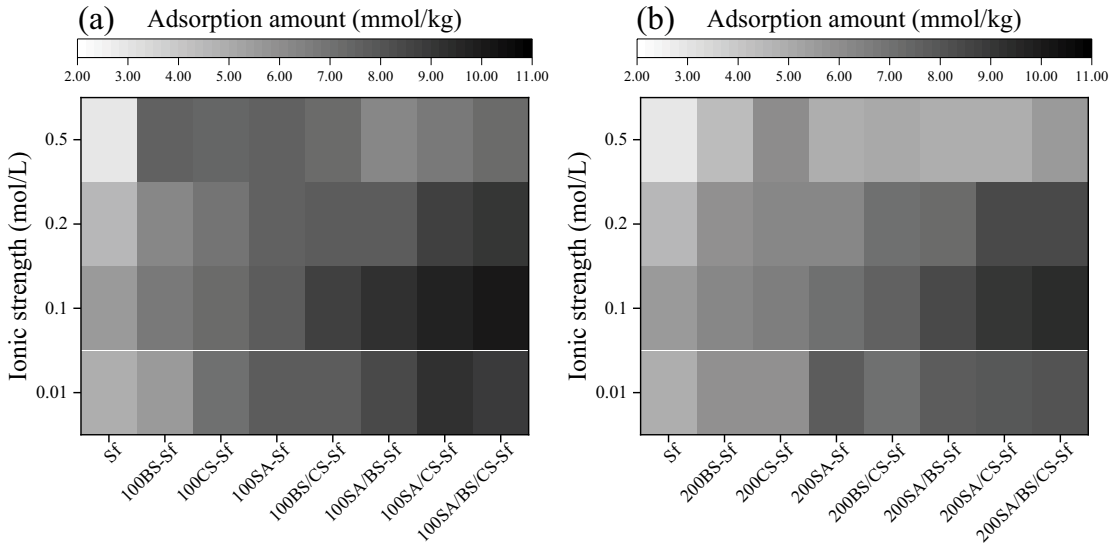

Fig. 4. Effect of ionic strength on oxytetracycline adsorption by 100% (a) and 200% (b) modified Sfs.

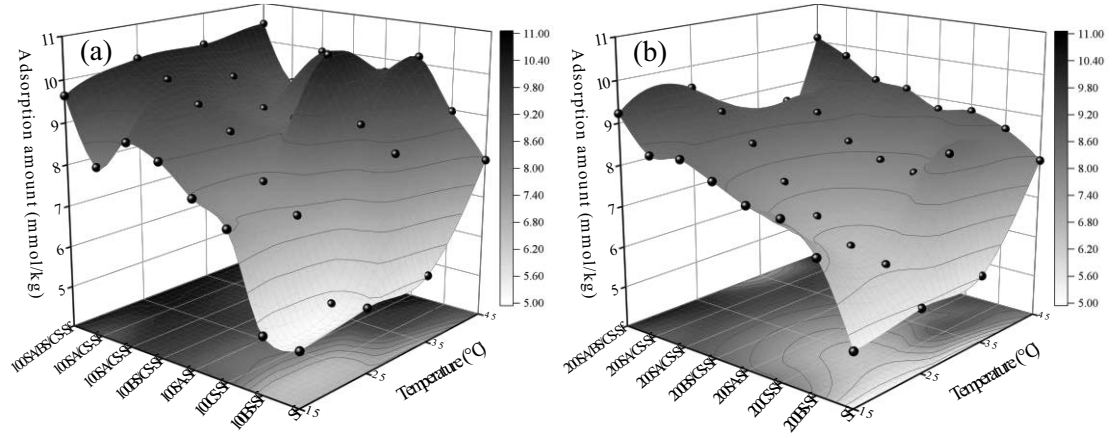

Fig. 5. Effect of temperature on oxytetracycline adsorption by 100% (a) and 200% (b) modified Sfs.

The adsorption kinetic curves of oxytetracycline on the modified Sfs was simulated using pseudo-first-order, pseudo-second-order, and Elovich kinetic equation models, and the fitting parameters of the adsorption kinetics are shown in Table 3. The adsorption kinetics of OTC conformed to the pseudo-second-order kinetic equation. The R^2 values of the pseudo-second-order kinetic equation for oxytetracycline adsorption were higher than those of the pseudo-first-order and Elovich kinetic equations. These results showed that the adsorption of OTC by the modified Sfs was primarily driven by chemisorption, consistent with the observed temperature effect. The equilibrium adsorption quantities obtained by the pseudo-second-order kinetic equations were larger than the equilibrium adsorption quantities calculated by the pseudo-first-order and Elovich kinetic equations and closer to the experimentally measured equilibrium adsorption amounts. This result indicated that the pseudo-second-order kinetic can describe the roles of pore filling, covalent bond formation, and electron exchange, which could reflect the adsorption of charcoal fiber materials to oxytetracycline quite effectively [37].

3.5. SEM and FTIR analysis of test materials

The SEM images of the different modified Sfs are shown in Fig. 7a–d. The original Sf had a smooth surface and a compact structure. After being modified by SA, the surface of SA-Sf became rough and loose. The degree of roughness and looseness on the surface of SA/BS-Sf further increased, and SA/BS/CS-Sf had remarkable roughness and looseness. The surface modification obviously demonstrated on the structural level and morphological traits of Sf. The most noticeable morphological and structural modifications of the material were those made by ternary modification, followed by binary and single modifications, consistent with the variation of the q_m. The FTIR spectra of the different modified Sfs are shown in Fig. 7e. After single and composite modifications, the structural groups in the different

Table 2
Thermodynamic parameters of oxytetracycline adsorption

Tested samples	Langmuir model				Henry model				Freundlich model			
	ΔG (kJ/mol)		ΔH (kJ/mol)	ΔS (kJ/mol·K)	ΔG (kJ/mol)		ΔH (kJ/mol)	ΔS (kJ/mol·K)	ΔG (kJ/mol)		ΔH (kJ/mol)	ΔS (kJ/mol·K)
	15°C	45°C			15°C	45°C			15°C	45°C		
Sf	–28.16	–31.16	8.75	108.27	–27.54	–30.63	8.48	125.02	–26.93	–29.85	8.21	121.97
100BS-Sf	–29.06	–32.42	9.63	111.87	–28.20	–30.96	7.45	123.73	–27.65	–30.90	8.88	126.77
100CS-Sf	–29.60	–32.46	8.07	102.88	–28.89	–31.26	6.30	122.13	–29.03	–31.85	7.41	126.44
100SA-Sf	–29.82	–32.41	7.16	98.10	–29.02	–31.61	6.82	124.39	–29.26	–31.82	6.69	124.75
100BS/CS-Sf	–30.55	–33.01	6.47	97.11	–29.45	–32.03	6.69	125.43	–29.88	–32.28	6.19	125.15
100SA/CS-Sf	–30.81	–33.28	6.45	97.33	–29.63	–32.22	6.69	126.04	–28.82	–31.15	6.20	121.54
100SA/BS-Sf	–31.05	–33.50	6.35	97.45	–29.99	–32.49	6.39	126.26	–30.50	–32.92	6.09	126.99
100SA/BS/CS-Sf	–31.69	–34.14	6.14	98.31	–30.58	–33.06	6.21	127.68	–31.17	–33.58	5.94	128.81
200BS-Sf	–23.03	–25.13	6.96	104.07	–28.43	–30.85	6.53	121.31	–27.88	–30.32	6.70	120.00
200CS-Sf	–22.89	–24.84	6.54	102.12	–28.59	–31.26	7.12	123.94	–28.07	–30.39	6.34	119.40
200SA-Sf	–21.50	–23.30	6.42	96.90	–29.18	–31.73	6.68	124.45	–28.93	–31.25	6.17	121.80
200BS/CS-Sf	–20.80	–22.55	6.44	94.54	–29.60	–31.78	5.66	122.38	–29.46	–31.82	6.15	123.57
200SA/CS-Sf	–21.10	–22.81	6.18	94.70	–29.44	–32.05	6.77	125.66	–29.75	–32.06	5.97	123.97
200SA/BS-Sf	–21.48	–23.37	6.73	97.90	–30.06	–32.39	5.96	125.01	–30.08	–32.58	6.36	126.48
200SA/BS/CS-Sf	–21.80	–23.57	6.22	97.27	–30.30	–32.68	6.04	126.12	–30.61	–33.00	6.00	127.05

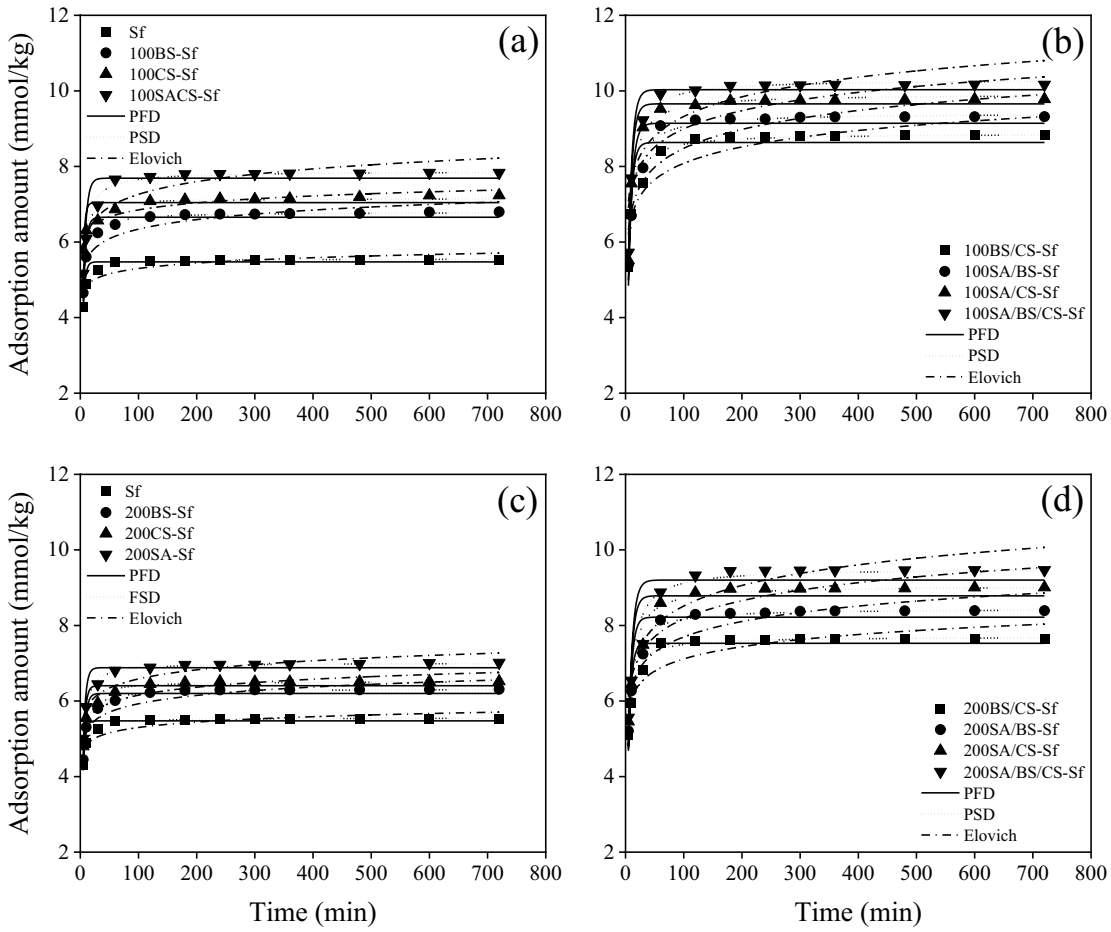

Fig. 6. Adsorption kinetics of oxytetracycline by 100% (a,b) and 200% (c,d) modified Sfs.

Table 3
Fitting parameters of adsorption kinetics for oxytetracycline

Tested samples	Pseudo-first-order kinetic equation		Pseudo-second-order kinetic equation		Elovich equation	
	q_e (mmol/kg)	R^2	q_e (mmol/kg)	R^2	q_e (mmol/kg)	R^2
Sf	5.47	0.8987**	5.55	0.9967**	4.86	0.7737**
100BS-Sf	6.66	0.9105**	6.79	0.9960**	2.74	0.8250**
100CS-Sf	7.04	0.7246**	7.15	0.9389**	3.75	0.9188**
100SA-Sf	7.69	0.8793**	7.87	0.9888**	2.06	0.8282**
100BS/CS-Sf	8.63	0.8849**	8.87	0.9849**	1.60	0.8453**
100SA/CS-Sf	9.14	0.9002**	9.41	0.9876**	1.38	0.8303**
100SA/BS-Sf	9.66	0.9758**	9.91	0.9885 **	1.43	0.7554**
100SA/BS/CS-Sf	10.03	0.9636**	10.3	0.9936**	1.33	0.7767**
200BS-Sf	6.20	0.8964**	6.32	0.9919**	3.13	0.8258**
200CS-Sf	6.41	0.8510**	6.52	0.9828**	3.28	0.8474**
200SA-Sf	6.88	0.8903**	7.01	0.9959**	2.88	0.8219**
200BS/CS-Sf	7.53	0.8738**	7.70	0.9849**	2.15	0.8158**
200SA/CS-Sf	8.22	0.8766**	8.44	0.9850**	1.70	0.8423**
200SA/BS-Sf	8.79	0.8409**	9.05	0.9722**	1.45	0.8675**
200SA/BS/CS-Sf	9.20	0.8057**	9.51	0.9545**	1.27	0.8842**

Note: **indicates significance at $P = 0.01$ level ($r = 0.765$ at $P = 0.01$ when the degree of freedom $f = 8$).

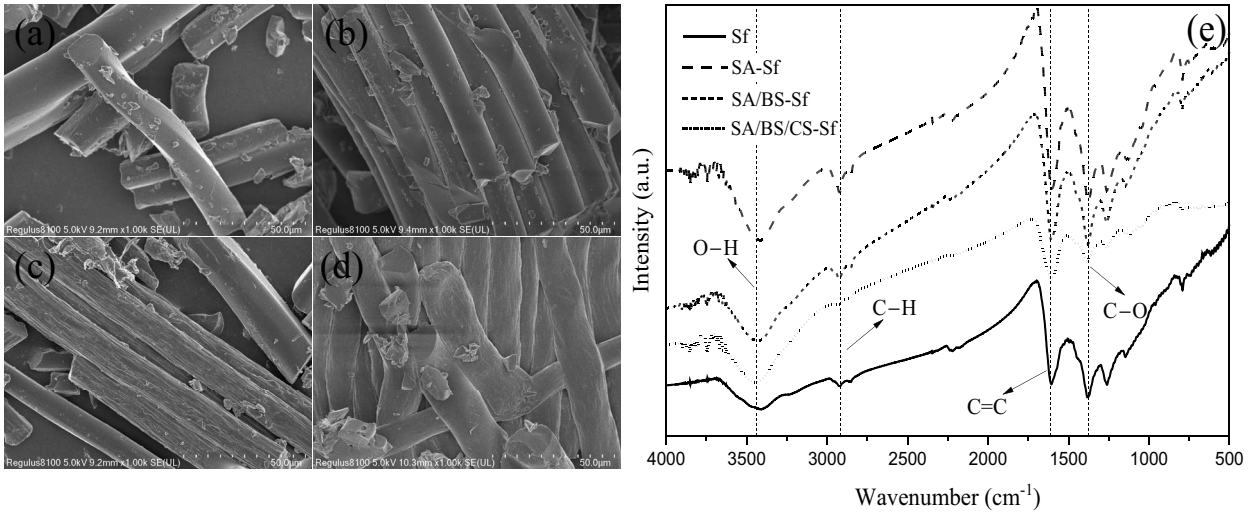

Fig. 7. Scanning electron microscopy images of Sf (a), 100SA-Sf (b), 100SA/BS-Sf (c), 100SA/BS/CS-Sf (d), and Fourier-transform infrared spectroscopy (e) of the four materials

modified Sfs showed no position variance of characteristic peaks, but the characteristic peak intensity was observably higher than that of raw Sf. The vibration wave number of about 1,300 cm^{-1} can be attributed to C–O single bond, indicating the presence of alcohol, phenol, ether, carboxylic acid, and lipid [36]. The wave number of around 3,400 cm^{-1} demonstrated an O–H stretching vibration absorption peak. The absorption peak of the wave number of around 1,632 and 2,900 cm^{-1} were mainly the characteristic peak of C=C and C–H stretching vibration. The peak intensities of modified Sfs at C=C, O–H, and C–H were stronger than those of raw Sf, whereas the intensities of other absorption peaks were similar to those of raw Sf.

3.6. Reusability of test materials

After the OTC-adsorption experiment, Sf, 100SA-Sf, 100SA/BS-Sf, and 100SA/BS/CS-Sf were regenerated with 5% nitric acid and ethanol with a regeneration time of 2 h. The mass loss of different materials and adsorption amount of OTC after three times of regeneration are shown in Fig. 8a and b, respectively. The mass loss of different materials reached 6.87%–10.86% after the first regeneration. With increased regeneration time, the mass loss of different materials gradually decreased, and the loss rate of the third regeneration was about 5.66%–7.58%. After one regeneration, the amount of OTC adsorbed onto different materials can

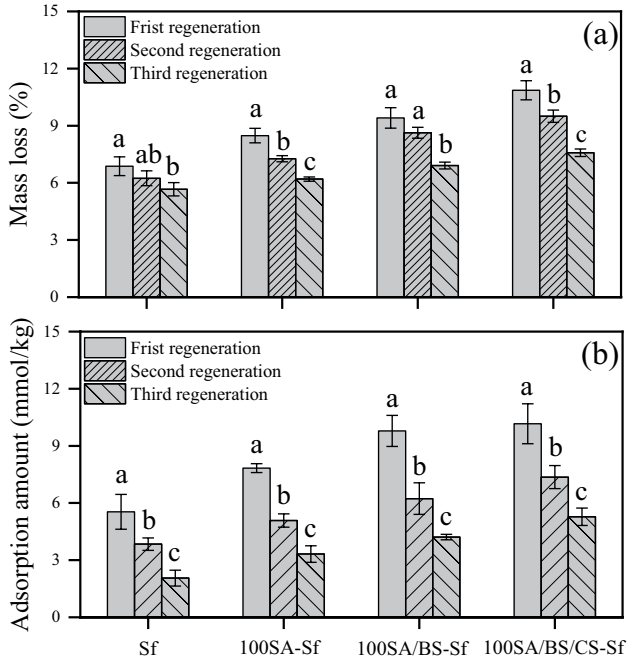

Fig. 8. Regeneration properties of the tested materials.

still reach about 70% of that on the non-regenerated materials. With increased regeneration time, the OTC adsorption amount decreased, and the decrease rate on 100SA/BS/CS-Sf was larger than that on the other materials. 100SA/BS/CS-Sf is a good cyclic- adsorption material whose adsorption effect can still reach about 50% of the original material after three times of regeneration, and had better regenerative capacity than that of amphoteric clay-loaded biochar [38].

4. Conclusion

In this study, the resource utilization of acrylic fiber was successfully realized, with high adsorption performance. Langmuir model can better fitted the adsorption isotherms of OTC than Henry and Freundlich models, with the q_m maintained at 16.11–65.25 mmol/kg. The q_m of OTC presented the trend of ternary > binary > single modification. The adsorption amount of OTC on different modified Sfs increased first and then decreased with increasing pH and ionic strength, reaching the maximum value at pH 5 and ionic strength of 0.1 mol/L. OTC adsorption on different modified Sfs increased with the increase in temperature, and the adsorption was a spontaneous, endothermic, and entropy-increasing process, which conformed to the pseudo-second-order kinetic equation. SEM and FTIR results proved that the modifiers were modified on the surface and that they changed the surface properties of Sf, and 100SA/BS/CS-Sf is a good cyclic-adsorption material.

Acknowledgements

The authors wish to acknowledge and thank the Sichuan transportation technology project (2021-ZL-8), the fundamental research funds of China west normal university (20A022), the education department of Sichuan province (18ZB0576), the scientific research foundation of Sichuan science and technology agency (2018JY0224), and the Tianfu scholar program of Sichuan province (2020–17).

Conflict of interests

The authors declare that they have no conflict of interest.

References

[1] A.D. Plessis, Persistent degradation: global water quality challenges and required actions, One Earth, 5 (2022) 129–131.
[2] C.O. Okoye, R. Nyaruaba, R.E. Ita, S.U. Okon, C.I. Addey, C.C. Ebido, A.O. Opabunmi, E.S. Okeke, K.I. Chukwudozie, Antibiotic resistance in the aquatic environment: analytical techniques and interactive impact of emerging contaminants, Environ. Toxicol., 96 (2022) 103995, doi: 10.1016/j.etap.2022.103995.
[3] J. Gao, L. Li, L. Duan, M. Yang, X. Zhou, Q. Zheng, Y. Ou, Z. Li, F.Y. Lai, Exploring antibiotic consumption between urban and sub-urban catchments using both parent drugs and related metabolites in wastewater-based epidemiology, Sci. Total Environ., 827 (2022) 154171, doi: 10.1016/j.scitotenv.2022.154171.
[4] C. Zhao, L. Xin, X. Xu, Y. Qin, W. Wu, Dynamics of antibiotics and antibiotic resistance genes in four types of kitchen waste composting processes, J. Hazard. Mater., 424 (2022) 127526, doi: 10.1016/j.jhazmat.2021.127526.
[5] J. Wang, L. Chu, L. Wojnárovits, E. Takács, Occurrence and fate of antibiotics, antibiotic resistant genes (ARGs) and antibiotic resistant bacteria (ARB) in municipal wastewater treatment plant: an overview, Sci. Total Environ., 744 (2020) 140997, doi: 10.1016/j.scitotenv.2020.140997.
[6] L. Chen, Q. Li, X. Xiao, T. Meng, Y. Zhang, Z. Wei, Y. Cao, Predicted non-effect concentration and risk assessment of typical tetracycline antibiotics, Asian J. Ecotoxicol., 16 (2021) 334–346.
[7] E.K. Putra, R. Pranowo, J. Sunarso, N. Indraswati, S. Ismadji, Performance of activated carbon and bentonite for adsorption of amoxicillin from wastewater: mechanisms, isotherms and kinetics, Water Res., 43 (2009) 2419–2430.
[8] H. Zhao, Z. Wang, Y. Liang, T. Wu, Y. Chen, J. Yan, Y. Zhu, D. Ding, Adsorptive decontamination of antibiotics from livestock wastewater by using alkaline-modified biochar, Environ. Res., 226 (2023) 115676, doi: 10.1016/j.envres.2023.115676.
[9] S. Liang, H. Zhang, H. Dai, X. Wan, F. Zhu, Q. Xu, W. Ji, Efficient, rapid and simple adsorption method by polydopamine polystyrene nanofibers mat for removal of multi-class antibiotic residues in environmental water, Chemosphere, 288 (2022) 132616, doi: 10.1016/j.chemosphere.2021.132616.
[10] J. Liu, H. Lin, Y. Dong, Y. He, W. Liu, Y. Shi, The effective adsorption of tetracycline onto MoS_2@Zeolite-5: adsorption behavior and interfacial mechanism, J. Environ. Chem. Eng., 9 (2021) 105912, doi: 10.1016/j.jece.2021.105912.
[11] Y. Sun, M. Chen, H. Liu, Y. Zhu, D. Wang, M. Yan, Adsorptive removal of dye and antibiotic from water with functionalized zirconium-based metal organic framework and graphene oxide composite nanomaterial Uio-66-$(OH)_2$/GO, Appl. Surf. Sci., 525 (2020) 146614, doi: 10.1016/j.apsusc.2020.146614.
[12] K. Rohit, S.R. Sharan, M. Devendra, Comparative study for sorption of arsenic on peanut shell biochar and modified peanut shell biochar, Bioresour. Technol., 375 (2023) 128831, doi: 10.1016/j.biortech.2023.128831.
[13] D. Cheng, H.H. Ngo, W. Guo, S.W. Chang, D.D. Nguyen, X. Zhang, S. Varjani, Y. Liu, Feasibility study on a new pomelo peel derived biochar for tetracycline antibiotics removal in swine wastewater, Sci. Total Environ., 720 (2020) 137662, doi: 10.1016/j.scitotenv.2020.137662.
[14] Z.T. Liu, J. Shao, Y. Li, Y.R. Wu, Y. An, Y.F. Sun, Z.H. Fei, Adsorption performance of tetracycline in water by alkali-modified wheat straw biochars, Chin. Environ. Sci., 42 (2022) 3736–3743.

[15] W. Hu, Y. Niu, K. Dong, D. Wang, Removal mechanism of typical antibiotics by bagasse biochar, Technol. Water Treat., 48 (2022) 52–56.
[16] J. Yu, H. Ding, Z.L. Zhang, Y. Li, L. Ding, Sorption characteristics and mechanism of oxytetracycline in water by modified biochar derived from chestnut shell, Chin. Environ. Sci., 41 (2021) 5688–5700.
[17] Y. Zhou, J.J. Shi, G.J. Qian, J.P. Hu, Z.L. Chen, Removal of amoxicillin from aqueous solution using Chinese's sugarcane bagasse biochar, J. Safe. Environ., 23 (2023) 268–277.
[18] H.Y. Deng, H.X. He, W.B. Li, T. Abbas, Z.F. Liu, Characterization of amphoteric bentonite-loaded magnetic biochar and its adsorption properties for Cu^{2+} and tetracycline, PeerJ., 10 (2022) e13030, doi: 10.7717/peerj.13030.
[19] Y. Zou, H.Y. Deng, M. Li, Y.H. Zhao, W.B. Li, Enhancing tetracycline adsorption by riverbank soils by application of biochar-based composite materials, Desal. Water Treat., 207 (2020) 332–340.
[20] Q. Yang, P. Wu, Preparation of modified porous biochar and its adsorption properties for tetracycline in water, J. Environ. Sci., 39 (2019) 3973–3984.
[21] Y. Ma, P. Li, L. Yang, L. Wu, L. He, F. Gao, X. Qi, Z. Zhang, Iron/zinc and phosphoric acid modified sludge biochar as an efficient adsorbent for fluoroquinolones antibiotics removal, Ecotoxicol. Environ. Saf., 196 (2020) 110550, doi: 10.1016/j.ecoenv.2020.110550.
[22] C. Duan, N. Zhao, X. Yu, X. Zhang, J. Xu, Chemically modified kapok fiber for fast adsorption of Pb^{2+}, Cd^{2+}, Cu^{2+} from aqueous solution, Cellulose, 20 (2013) 849–860.
[23] Y. Liu, X. He, X. Duan, Y. Fu, D.D. Dionysiou, Photochemical degradation of oxytetracycline: influence of pH and role of carbonate radical, Chem. Eng. J., 276 (2015) 113–121.
[24] P. Prarat, P. Hongsawat, P. Punyapalakul, Amino-functionalized mesoporous silica-magnetic graphene oxide nanocomposites as water-dispersible adsorbents for the removal of the oxytetracycline antibiotic from aqueous solutions: adsorption performance, effects of coexisting ions, and natural organic matter, Environ. Sci. Pollut. Res., 27 (2020) 6560–6576.
[25] H.N. Tran, E.C. Lima, R.S. Juang, J.C. Bollinger, H.P. Chao, Thermodynamic parameters of liquid–phase adsorption process calculated from different equilibrium constants related to adsorption isotherms: a comparison study, J. Environ. Chem. Eng., 9 (2021) 106674, doi: 10.1016/j.jece.2021.106674.
[26] R. Acosta, V. Fierro, A. Martinez de Yuso, D. Nabarlatz, A. Celzard, Tetracycline adsorption onto activated carbons produced by KOH activation of tyre pyrolysis char, Chemosphere, 149 (2016) 168–176.
[27] Y.F. Wang, H.Y. Deng, W.B. Li, A. Touqeer, M. Li, J.N. Wu, J.M. Ouyang, Litter extract from *Alternanthera philoxeroides* as an efficient passivator for oxytetracycline stability in riverbank purple soils, Environ. Technol. Innovation, 29 (2023) 103022, doi: 10.1016/j.eti.2023.103022.
[28] Z.W. Zhao, C. Chen, Z.J. Liang, F.Y. Cui, Enhanced adsorption activity of manganese oxide-modified biochar for the removal of tetracycline from aqueous solution, J. Agro-Environ. Sci., 40 (2021) 194–201.
[29] H. Maria, G. Ciobanu, Studies on adsorption of oxytetracycline from aqueous solutions onto hydroxyapatite, Sci. Total Environ., 628/629 (2018) 36–43.
[30] W.B. Li, S.N. Zhou, H.Y. Deng, A. Touqeer, Performance comparison of Mg-loaded amphoteric clays in antibiotics adsorption from aqueous solutions, Desal. Water Treat., 278 (2022) 159–168.
[31] Y. Sun, Q. Yue, B. Gao, Q. Li, L. Huang, F. Yao, X. Xu, Preparation of activated carbon derived from cotton linter fibers by fused NaOH activation and its application for oxytetracycline (OTC) adsorption, J. Colloid Interface Sci., 368 (2012) 521–527.
[32] Y. Gao, Y. Li, L. Zhang, H. Huang, J. Hu, S.M. Shah, X. Su, Adsorption and removal of tetracycline antibiotics from aqueous solution by graphene oxide, J. Colloid Interface Sci., 368 (2012) 540–546.
[33] Y. Qiu, Z. Zheng, Z. Zhou, G.D. Sheng, Effectiveness and mechanisms of dye adsorption on a straw-based biochar, Bioresour. Technol., 100 (2009) 5348–5351.
[34] F. Saremi, M.R. Miroliaei, M.S. Nejad, H. Sheibani, Adsorption of tetracycline antibiotic from aqueous solutions onto vitamin B6-upgraded biochar derived from date palm leaves, J. Mol. Liq., 318 (2020) 114126, doi: 10.1016/j.molliq.2020.114126.
[35] P. Huang, C. Ge, D. Feng, H. Yu, J. Luo, J. Li, P.J. Strong, A.K. Sarmah, N.S. Bolan, H. Wang, Effects of metal ions and pH on ofloxacin sorption to cassava residue-derived biochar, Sci. Total Environ., 616–617 (2018) 1384–1391.
[36] W.B. Li, M.T. Guo, Y.F. Wang, H.Y. Deng, H. Lei, C.T. Yu, Z.F. Liu, Selective adsorption of heavy metal ions by different composite-modified semi-carbonized fibers, Sep. Purif. Technol., 328 (2023) 125022, doi: 10.1016/j.seppur.2023.125022.
[37] A.R. Lucaci, D. Bulgariu, I. Ahmad, G. Lisă, A.M. Mocanu, L. Bulgariu, Potential use of biochar from various waste biomass as biosorbent in Co(II) removal processes, Water, 11 (2019) 1565, doi: 10.3390/w11081565.
[38] W.B. Li, H.Y. Deng, Y. Ye, S.N. Zhou, A. Touqeer, J.M. Ouyang, Q. Kuang, W. Liu, Effect of pH on adsorptive and cycling performance of amphoteric clay-loaded biochar, Desal. Water Treat., 264 (2022) 111–120.